직접탄소 연료전지용 LSM/GDC 공기극 지지체 제조 및 전기화학 특성 평가

빌랄 아메드[1,2] · 완디 와휴디[1,2] · 이승복[1,2†] · 송락현[1,2] · 이종원[1,2] · 임탁형[2] · 박석주[2]

[1]과학기술연합대학원 신에너지학과, [2]한국에너지기술연구원 수소연료전지연구단

Fabrication and Electrochemical Characterization of LSM/GDC based Cathode Supported Direct Carbon Fuel Cells

BILAL AHMED[1,2], WANDI WAHYUDI[1,2], SEUNG-BOK LEE[1,2†], RAK-HYUN SONG[1,2],

JONG-WON LEE[1,2], TAK-HYOUNG LIM[2], SEOK-JOO PARK[2]

[1]Department of Advanced Energy Technology, University of Science and Technology,
217 Gajeong-ro Yuseong-gu, Daejeon, Korea
[2]Fuel Cell Research Center, Korea Institute of Energy Research, 102 Gajeong-ro, Yuseong-gu, Daejeon, Korea

Abstract >> In this study, successive coating and co-sintering techniques have been used to fabricate LSM/GDC based cathode supported direct carbon fuel cells. The porous LSM/GDC cathode substrate, dense, thin and crack free GDC and ScSZ layers as bi-layer electrolyte, and a porous Ni/ScSZ anode layer was obtained by co-firing at 1400℃. The porous structure of LSM/GDC cathode substrate, after sintering at 1400℃, was obtained due to the presence of GDC phase, which inhibits sintering of LSM because of its higher sintering temperature. The electrochemical characterization of assembled cell was carried out with air as an oxidant and carbon particles in molten carbonate as fuel. The measured open circuit voltages (OCVs) were obtained to be more than 0.99 V, independent of testing temperature. The peak power densities were 116, 195 and 225 mW cm^{-2} at 750, 800 and 850℃, respectively.

Key words : LSM, GDC, Composite cathode(복합 공기극), Cathode-supported(공기극지지체), Direct carbon fuel cell(직접 탄소 연료전지)

1. Introduction

The two major problems of tomorrow's world will be energy and pollution, and an efficient utilization of current energy resources in an eco-friendly way

has attracted much attention[1,2]. The trend-setter energy economies like US and China has extensive coal reserves, so expectedly, coal is going to be the dominant fuel in the coming few years. Therefore, it is substantial to develop clean and efficient coal conversion technology. Along with this potential, direct carbon fuel cells (DCFCs) has regained research focus because of their numerous advantages e.g. 100% thermodynamic efficiency and fuel availability[3-6].

DCFC uses solid carbon as fuel and electrochemically converts its chemical energy into electricity without combustion or gasification. This direct conversion of solid carbon eliminates SO_x and NO_x emissions and minimizes CO_2 emission. Based on electrolyte, DCFC can be divided into three categories; molten hydroxide, molten carbonate and solid oxide electrolyte[5, 7-12].

Recently, solid oxide based direct carbon fuel cell (SO-DCFC) has gained considerable research interests due to faster kinetics and eradication of problems caused by liquid electrolytes. But, the research about SO-DCFCs is at an early stage and very few published reports available. The conventional anode-supported SO-DCFC had been reported by Liu et al.[13] but this configuration faced two major problems; firstly, because of close ended fuel electrode, fuel supply cannot be continuous, secondly, concentration losses because of thicker fuel electrode[14]. Cathode-supported design provides solution to these fundamental issues. In solid oxide fuel cells (SOFCs), cathode-supported designs are considered as structurally stable because they do not undergo through the redox cycle like Ni-YSZ anode-supported cells. Also, because vapors are not formed at the cathode, the size of its pores can be smaller than those of the anode supports, and therefore it can be thinner than an anode with the same mechanical strength[15].

In this study, we used LSM/GDC composite as cathode support and cathode supported button cells were fabricated by successive coating and co-firing techniques. The coin cells were tested in both SOFC and DCFC mode and preliminary results showed that this schematic has potential to be optimized in future work.

2. Experimental

2.1 Button Cell Preparation

Commercially available $La_{0.8}Sr_{0.2}MnO_{3-d}$ (LSM; Fuel Cell Materials, USA) and $Gd_{0.1}Ce_{0.9}O_{2-d}$ (Gadolinia doped Ceria, GDC; Fuel Cell Materials, USA) powders were mixed in desired weight ratio along with graphite powder and ball milled with ethanol for 48 hrs. After drying and sieving, LSM/GDC powder was shaped into circular discs by uniaxial pressing. LSM/GDC support was pre-sintered at 1200℃, followed by GDC interlay coating via vacuum slurry coating technique. GDC interlayer was co-fired at 1100℃ prior to ScSZ electrolyte layer coating. After ScSZ electrolyte layer, Ni/ScSZ anode layer was screen printed and the whole cell assembly was co-fired at 1400℃ for five hours. The final dimensions of the resulting cells were 20 mm diameter and 1.5 mm thickness and the effective anode and cathode area was 1.0 cm^2. The thickness of bi-layer electrolyte is less than 10 μm and thickness of anode layer varies from 25 to 35 μm.

2.2 Cell Characterization

In order to examine the chemical compatibility of LSM and GDC powders during high temperature sintering, X-ray diffraction (XRD) patterns were measured using an automated Rigaku diffractometer (2500 D/MAX; Rigaku, Japan) with Cu-K$_α$ radiation. The data was recorded over a scanning angle range of 20° to 80° using a step width of 0.025° and a holding time of 5 s. After co-firing, microstructure of button cell layers was observed using scanning electronic microscopy (S-4700; Hitachi Ltd., Japan).

Ag meshes and Ag wires were used as current collectors and attached to the electrodes with a

ceramic binder. Pt paste was used to reduce contact resistance. The cells were assembled to an alumina tube and sealed with the ceramic paste to separate anode and cathode compartment. In SOFC mode, humidified hydrogen (0.1 L/min) and air (0.2 L/min) were supplied to the anode and cathode sides, respectively. In DCFC mode, 5.0 g of carbon black fuel mixed with molten carbonate was fed into anode compartment and air (0.2 L/min) supplied to cathode side. Cell performance was measured at various temperatures between 700 and 850℃. Impedance spectra was obtained with SI1287 and SI 1260 equipment (Solartron Instruments, UK) vs. open circuit voltage (OCV) with an amplitude of 10 mV at a frequency between 0.1 and 10000 Hz.

3. Results and Discussions

3.1 Phase Stability

The XRD patterns of the pure LSM, pure GDC and sintered mixture of LSM and GDC are presented in Fig. 1. The pure LSM exhibited a perovskite phase structure with rhombohedral symmetry while pure
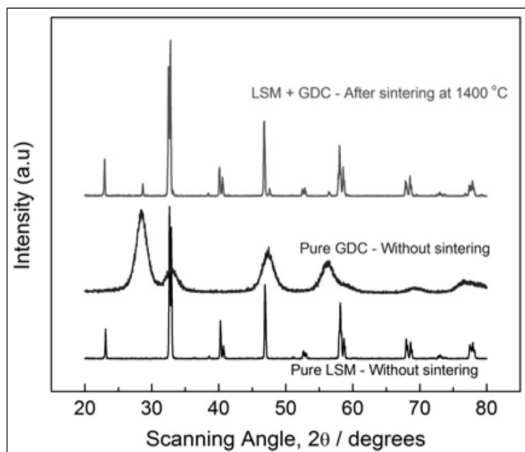

Fig. 1 X-ray diffraction patterns of the pure LSM (without sintering), pure GDC (without sintering) and LSM/GDC mixture after co-firing at 1400℃

GDC showed fluorite type structure. The most important feature is that all peaks of mixture of LSM and GDC correspond to either LSM or GDC. This feature indicates that LSM and GDC do not form any secondary phases during high temperature sintering.

3.2 SEM Microscopy

Fig. 2a presents the schematic design of LSM/
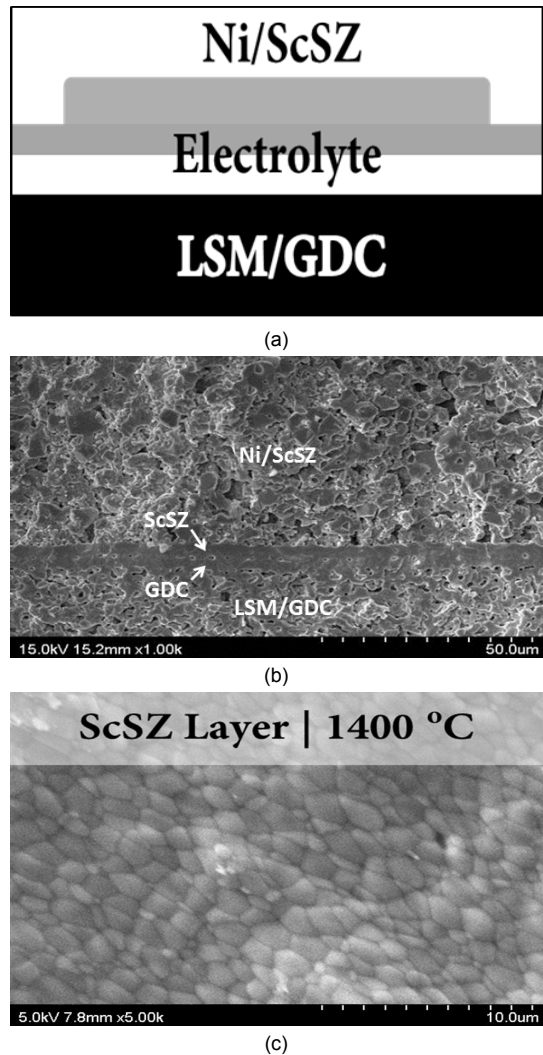

(a)

(b)

(c)

Fig. 2 (a) schematic design of LSM/GDC based cathode supported button cell, (b) cross-sectional view of co-fired cathode supported cell and (c) surface morphology of ScSZ electrolyte after co-firing at 1400℃

GDC based cathode-supported button cell. The electrolyte consists of two layer; GDC and ScSZ where GDC act as buffer layer between cathode and ScSZ layer act as an ion-conduction electrolyte at high operating temperature. Total thickness of bi-layer electrolyte is less than 10 μm which is desirable to minimize electrolyte resistance. Fig. 2b shows the cross-sectional view of cell after co-firing at 1400℃ for five hours. Porous anode and cathode layer are mentioned as Ni/ScSZ and LSM/GDC, respectively. Thin, dense and crack free bi-layer electrolyte of GDC and ScSZ is shown. Though, some pin holes are present between GDC and ScSZ layer but as long as they are closed, they are not going to create any problem during cell operation. Also, electrode/electrolyte interfaces are well adherent along with porous cathode and anode. The surface morphology of ScSZ electrolyte layer after co-firing at 1400℃ is presented in Fig. 2c. Crack free and dense nature of ScSZ layer is exactly according to electrolyte requirements.

3.3 Electrochemical Characterization:

The current-voltage (I-V) and current-power density (I-P) curves for the cathode-supported coin cells, with hydrogen as fuel and air as an oxidant, are presented in Fig. 3. The cell showed quite impressive power densities like 291, 383 and 450 mW cm^{-2} at 750, 800 and 850℃, respectively. The observed open circuit voltages are close to the theoretically predicted values of open circuit voltage, which indicates that electrolyte is fairly dense because electrolyte leakage leads to the severe drop of open circuit voltage of cell. The power density of cell is affected by cathode support thickness and it can be optimized by changing microstructure and reducing interfacial contact resistance.

Fig. 4 presents the current-voltage (I-V) and current-power density (I-P) curves of cathode-supported
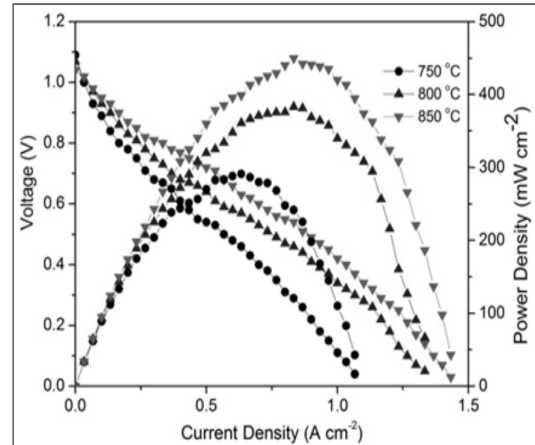

Fig. 3 Current voltage (I-V) and current-power density (I-P) curves for cathode supported button cells in SOFC mode at different temperatures
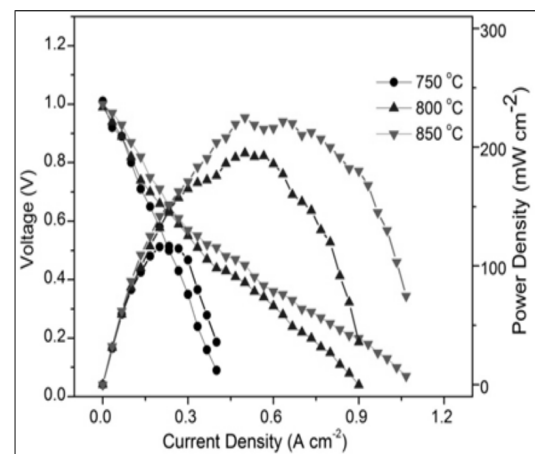

Fig. 4 Current voltage (I-V) and current-power density (I-P) curves for cathode supported button cells in DCFC mode at different temperatures

button cell in DCFC mode, with carbon particles in molten carbonate as fuel and air as an oxidant. The direct carbon fuel cell showed promising performance with the peak power densities of 117, 195 and 225 mW cm^{-2} at 750, 800 and 850℃, respectively.

The electrical impedance spectra measured under open circuit voltage conditions, at different temperatures, is presented in Fig. 5a and 5b for SOFC and DCFC mode, respectively. The ohmic resistance and
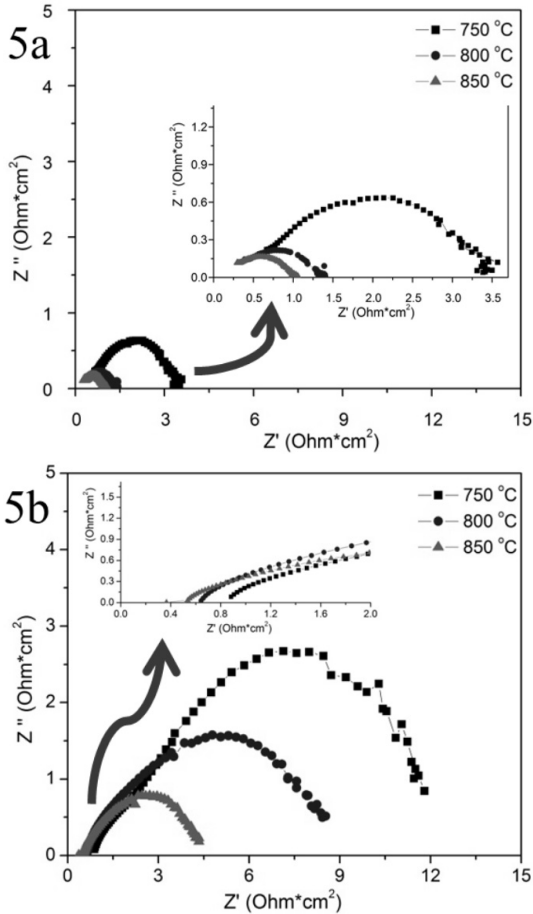
Fig. 5 Electrical impedance spectra for cathode supported button cells (a) in SOFC mode, (b) in DCFC mode

Table 1 Ohmic resistance (R_o), electrode polarization resistance (R_p) and total cell resistance (R_t) determined from impedance spectra of cathode supported button cell measured under open circuit voltage conditions at different temperature (a) in SOFC mode, (b) in DCFC mode

		750℃	800℃	850℃
R_o (Ohm.cm^2)	(a)	0.66	0.39	0.29
	(b)	0.88	0.64	0.51
R_p (Ohm.cm^2)	(a)	2.90	1.01	0.76
	(b)	10.91	7.88	3.85
R_t (Ohm.cm^2)	(a)	3.56	1.40	1.05
	(b)	11.79	8.53	4.33

total electrode polarization constitute the impedance spectra. The total ohmic resistance (R_o) of the cell consists of ionic resistance of the electrolyte layers, electronic resistance of both electrodes and interfacial contact resistance which is given by high frequency intercept of impedance spectra[16]. As, electrolyte layer contributes major part of R_o because electrode materials and interconnecters usually have small electronic resistance, so their resistance can be ignored[17]. Also, total cell polarization (R_t) is given by low frequency intercept therefore difference between low frequency and high frequency intercept is called electrode polarization resistance (R_p). These resistances data is summ-

arized in Table 1. Impedance data shows that cell performance is mainly effected by electrode polarization resistance which is far higher in DCFC mode as compared to SOFC mode. Electrode polarization resistance consists of the cathodic and anodic polarization resistance but in cathodesupported schematic, its mainly because of cathode because of its higher thickness and causing concentration losses. Interestingly, contribution of electrode polarization resistance to the overall cell resistance (R_p/R_t) is independent of temperature and in most of the cases its around 90%. Further investigation are required to determine cathodic and anodic contribution to the R_p values but up till this point, the reported results are very significant and has potential to be improved by more experiments. The cell resistance can be decreased by reducing cathode thickness and contact resistance between cathode substrate and electrolyte layer.

4. Conclusions

In the present work, LSM/GDC based cathode supported direct carbon fuel cells were electrochemically characterized. The cathode-supported button cells were co-fired at 1400℃ and XRD analysis after sintering proves that LSM and GDC are chemically compatible and there is no formation of secondary

phases during high temperature sintering. SEM images confirmed the presence of desired microstructure; porous cathode substrate layer, dense electrolyte layers and porous anode layer. LSM/GDC based cathode supported DCFC showed excellent performance and the electrochemical results show that fabricated cells are promising and results can be optimized by improving cathode structure and reducing interfacial resistance.

Acknowledgement

References

1. L. Schipper, Automobile use, fuel economy and CO_2 emissions in industrialized countries: Encouraging trends through 2008, Tranport Policy, Vol. 18, No. 2, 2011, pp. 358-372.

2. J. E. Sinton, D. G. Fridley, What goes up: recent trends in China's energy consumption, Energy Policy, Vol. 28, No. 10, 2000, pp. 671-687.

3. K. Pointon, B. Lakeman, J. Irvine, J. Bradley, S. Jain, The development of a carbon–air semi fuel cell, J. Power Sources, Vol. 162, No. 2, 2006, pp. 750-756.

4. N. J. Cherepy, R. Krueger, K. J. Fiet, A. F. Jankowski, J. F. Cooper, Direct conversion of carbon fuels in a molten carbonate fuel cell, J. Electrochem. Soc., Vol. 152, No. 1, 2005, pp. A80-A87.

5. M. Steingberg, Conversion of fossil and biomass fuels to electric power and transportation fuels by high efficiency integrated plasma fuel cell (IPFC) energy cycle, Int. J. Hydrogen Energy, Vol. 31, No. 3, 2006, pp. 405-411.

6. W. H. A. Peelen, K. Hemmes, J. H. W. de Wit, Carbon a major energy carrier for the future Direct carbon fuel cells and molten salt coal/ biomass gasification, High Temperature Material Processes, Vol. 2, No. 4, 1998, pp. 471-482.

7. G. A. Hackett, J.W. Zondlo, R. Svensson, Evaluation of carbon materials for use in a direct carbon fuel cell, J. Power Sources, Vol. 168, No. 1, 2007, pp. 111-118.

8. S. L. Jain, Y. Nabae, B. J. Lakeman, K. D. Pointon, J. T. S. Irvine, Solid state electrochemistry of direct carbon/air fuel cells, Solid State Ionics, Vol. 179, No. 27-32, 2008, pp. 1417-1421

9. S. Zecevic, E. M. Patton, P. Parharni, Carbon–air fuel cell without a reforming process, Carbon, Vol. 42, No. 10, 2004, pp. 1983-1993.

10. J. R. Selman, Molten-salt fuel cells—Technical and economic challenges, J. Power Sources, Vol. 160, No. 2, 2006, pp. 852-857.

11. T. Nunoura, K. Dowaki, C. Fushimi, S. Allen, E. Meszaros, M. J. Antal, Performance of a first-generation, aqueous-alkaline biocarbon fuel cell, Industrial and Engineering Chemistry Research, Vol. 46, No. 3, 2007, pp. 734-744.

12. X. Li, Z. H. Zhu, J. L. Chen, R. De Marco, A. Dicks, J. Bradley, G. Q. Lu, Characterization and biodegradation of chitosan-alginate polyelectrolyte complexes, Polymer Degradation and Statbility, Vol. 94, No. 1, 2009, pp. 1-6.

13. R. Z. Liu, C. H. Zhao, J. L. Li, F. R. Zeng, S. R. Wang, T. L. Wen, Z. Y. Wen, A novel direct carbon fuel cell by approach of tubular solid oxide fuel cells, J. Power Sources, Vol. 195, No. 2, 2010, pp. 480-482.

14. J. Zhou, X. F. Ye, L. Shao, X. P. Zhang, J.Q. Qian, S.R. Wang, A promising direct carbon fuel cell based on the cathode-supported tubular solid oxide fuel cell technology, Electrochimica Acta, Vol. 74, 2012, pp. 267-270.

15. S.C. Singhal, K. Kindall, High temperature solid

oxide fuel cells fundamentals. Design and application. Elsevier, Amstermdam (2003).

16. K. J. Yoon, W.H. Huang, G. S. Ye, S. Gopalan, U. B. Pal, D. A. Seccombe, Electrochemical performance of solid oxide fuel cells manufactured by single step co-firing process, Vol.

154 No. 4, 2007, pp. B389-B395.

17. L. Zhang, S. P. Jiang, W. Wang, Y. J. Zhang, NiO/YSZ anode-supported thin-electrolyte solid oxide fuel cells fabricated by gel casting, Vol. 170, No. 1, 2007, pp. 55-60.